The adsorption of Mn(II) by insolubilized humic acid

Wenlin Zhao, Bozhi Ren, Andrew Hursthouse and Feng Jiang

ABSTRACT

The eco-friendly and non-toxic natural organic substance, insolubilized humic acid (IHA), was used to remove Mn(II) from aqueous solutions. The adsorption characteristics were studied through a series of static adsorption tests. The results show that conditions such as the dose, the pH of the solution and the initial concentration of Mn(II) all affect removal efficiency, and the optimal pH value was 5.5. The sorption process for Mn(II) on IHA conforms to the pseudo-second-order adsorption kinetic model and intra-particle diffusion is not the only factor affecting the adsorption rate. Both Langmuir and Freundlich models can describe this adsorption behavior, and the experimental maximum adsorption capacity of IHA was 52.87 mg/g under optimal conditions. The thermodynamic analysis of adsorption shows that the adsorption process is a non-spontaneous endothermic physical reaction. Fourier transform infrared spectroscopy (FTIR), scanning electron microscopy (SEM) and energy-dispersive spectroscopy (EDS) were used to characterize the samples, it was found that as IHA successfully adsorbed Mn(II), the surface morphology of IHA changed after the adsorption reaction. The adsorption mechanism for Mn(II) on IHA is to provide electron pairs for carboxyl, phenolic hydroxyl and other functional groups to form stable complexes with Mn(II).

Key words | adsorption characteristics, adsorption isotherms, adsorption kinetics, insolubilized humic acid, Mn(II)

Wenlin Zhao
Bozhi Ren (corresponding author)
Andrew Hursthouse
Feng Jiang
School of Civil Engineering,
Hunan University of Science and Technology,
Xiangtan, 411201,
China
E-mail: *bozhiren@126.com*

Wenlin Zhao
Bozhi Ren
Feng Jiang
Hunan Provincial Key Laboratory of Shale Gas Resource Exploitation,
Xiangtan, 411201,
China

Andrew Hursthouse
Computing Engineering & Physical Sciences,
University of the West of Scotland,
Paisley PA1 2BE,
UK

HIGHLIGHTS

- Insoluble humic acid is a component of natural organic substances that is widely distributed.
- It has the advantage of being environmentally benign, of low toxicity and cost, and contains a variety of functional chemical groups.
- Chemisorption governs the removal of Mn(II) with q_m reaching 52.87 mg/g.

GRAPHICAL ABSTRACT

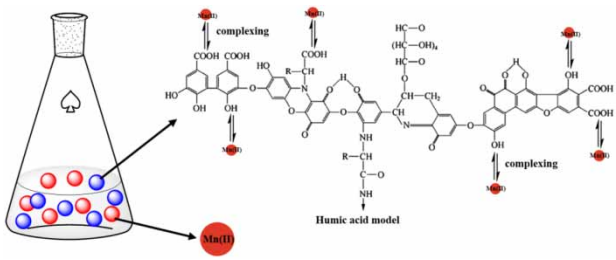

doi: 10.2166/wst.2020.384

INTRODUCTION

Industrial wastewater and mine drainage are an important source of pollution from potentially toxic elements (PTEs). These elements entering the environment are fixed or enriched by physical or chemical interactions with organic matter in water, which affects their morphology, migration, transformation and wider ecotoxicity (Li *et al.* 2013a; Lan *et al.* 2017). There are two types of bonding according to the properties of organic matter and metal ions (Schulten & Schnitzer 1993): one is the formation of an ionic bond to alkali metal ions such as Na(I), K(I), and another is the generation of complexes with heavy metal ions such as Cu(II), Pb(II) and Cd(II). There has been a lot of research on the reaction mechanism between organic matter and heavy metal ions such as Cu(II), Pb(II), Cd(II), Zn(II), etc. (El-Eswed & Khalili 2006; Oldham *et al.* 2017), but on the mechanism of interaction between organic matter and manganese is still scarce. The manganese ion is extremely unstable and harmful in water. If the human body absorbs too much manganese, it will cause poisoning and affect the central nervous system. In severe cases, it can cause irritability, hallucinations, and so on, resulting in manganese mania (He *et al.* 2005; Jiang *et al.* 2018). The World Health Organization (WHO) limits the maximum concentration of manganese in drinking water to 0.5 mg/L. At present, the treatment methods for manganese-containing wastewater mainly include chemical oxidation, bioremediation, electrolysis, adsorption and coagulation sedimentation (Patil *et al.* 2016; Yong *et al.* 2017; Hou *et al.* 2020). Among them, the adsorption method has the characteristics of easy operation, fast reaction speed, no introduction of other chemical substances, and avoiding secondary pollution, so it has a good application prospect (Huang *et al.* 2019).

Humic acid is widely distributed as a component of natural organic substances. As a potential material for water treatment, it has the advantage of being environmentally benign, of low toxicity and cost, and containing a variety of functional chemical groups, such as carboxyl, alcoholic hydroxyl, phenolic hydroxyl, aldehyde, ketone, and ethers (Manzak *et al.* 2017). The existence of these active groups determines a high reactivity with metal ions in aqueous solution through adsorption or complexation. When manganese ions in the water interact with the functional groups of humic acid, they will be adsorbed in the network structure of the humic acid macromolecule to form manganese-humic acid complexes (Oldham *et al.* 2017), strongly stabilized. Fawwaz Khalili *et al.* (Khalili & Al-Banna 2015) extracted insolubilized humic acid (NaIHA) from local soil to characterize it, and explored its adsorption properties for radioactive elements U(VI) and Th(IV). It is found that the adsorption characteristics of NaIHA for two metal ions conform to the Langmuir, Freundlich and Dubinin-Radushkevich (D-R) adsorption isotherm models, and the adsorption mechanisms include electrostatic adsorption and coordination. Li Chen *et al.* (Chen *et al.* 2020) investigated the adsorption-desorption characteristics of humic acid colloid (HAC) for vanadium (V) and the interaction between them through a series of experiments. It was found that six groups on HAC participated in V(V) adsorption, the adsorption process follows the Langmuir isotherm adsorption model and first-order kinetic model. However, high solution pH (7–11) and temperature (20–40 °C) will greatly reduce HAC adsorption capacity.

In this study, eco-friendly and non-toxic insoluble humic acid (IHA) was used as adsorbent to remove Mn(II) from aqueous solution. While exploring the adsorption effect and mechanism, a low-cost and efficient method for the treatment of manganese-containing industrial wastewater was also proposed. The effects of factors such as initial Mn(II) concentration, pH and the dose of IHA on Mn(II) adsorption by IHA were studied. The adsorption kinetics and model for isothermal adsorption of manganese on IHA were investigated. Solid phase characterization methods such as FTIR, SEM, and EDS were used to study the interaction between humic acid and metal manganese ions.

MATERIALS AND METHODS

Materials

All chemicals used in this study were of analytical grade and were not further purified before use. All solutions were made up with deionized water. Insolubilized humic acid and manganese(II) sulfate monohydrate ($MnSO_4{\cdot}H_2O$) were purchased from Sinopharm Chemical Reagent Co., Ltd (China, Shanghai). Hydrochloric acid (HCl) and sodium hydroxide (NaOH) were purchased from XiLong Science Co., Ltd (Shantou, China).

Batch adsorption experiment

The batch adsorption experiment was performed to determine the optimal conditions for the removal of Mn(II)

from the aqueous solution by IHA and to explore its adsorption characteristics. Stock solutions of Mn(II) were prepared by dissolving manganese(II) sulfate monohydrate with deionized water, which was stored in cold storage away from light, subsequent adsorption experiments with different concentrations of Mn(II) simulating surface water samples were to a reserve solution made according to a certain ratio dilution. A certain amount of IHA was added to a series of 250 mL conical flasks, then a certain volume of a known concentration of Mn(II) solution was added, and the pH adjusted to 2.5–7.5 with HCl and NaOH solution (0.25 M). Adsorption experiments were performed at a fixed speed of 160 rpm on the thermostatic oscillating incubator shaker with adjustable temperature. After the reaction, the mixed solution was filtered through a 0.45 μm filter membrane, and then the concentration of Mn(II) in the filtrate was measured with a flame atomic absorption spectrometer. The removal rate R(%) of Mn(II) and the adsorption capacity (q_t, q_e (mg/g)) at any time t of the adsorption reaction and the equilibrium of the adsorption in the adsorption experiments of each group were calculated with the equations below:

$$R(\%) = \frac{C_0 - C_e}{C_0} \times 100 \quad (1)$$

$$q_t = \frac{(C_0 - C_t) \cdot V}{m} \quad (2)$$

$$q_e = \frac{(C_0 - C_e) \cdot V}{m} \quad (3)$$

where C_0, C_e, and C_t represent the concentration (mg/L) of Mn(II) in the solution at the initial, equilibrium and any time, respectively; V is the volume (L) of Mn(II) solution and m is the dose of IHA (g).

Solid phase characterization

The IHA before and after adsorption of Mn(II) was dried and milled, and then KBr powder with a mass ratio of about 100:1 was added; after the mixture was fully milled again, it was pressed, and the FTIR spectra of the samples were recorded by Thermo Fisher Scientific Nicolet 6700 FTIR spectrometer instrument in the scanning range of 400–4,000 cm^{-1}. SEM-EDS was obtained from Hitachi S-4800 scanning electron microscopy, which is also equipped with an energy dispersive spectroscope.

RESULTS AND DISCUSSION

Effect of pH on Mn(II) removal

The insolubilized humic acid, with a dry weight of 1.00 g, was added to a 200 ml simulated water sample with a Mn(II) mass concentration of 100 mg/L. At a temperature of 298.15 K, the effect of pH (2.5–7.5) on Mn(II) adsorption by IHA was investigated (Figure 1).

It can be seen from the figure that with the increase of pH, the removal efficiency and adsorption capacity of Mn(II) gradually increased, from 23.17% to 61.69%, and 6.67 mg/g to 17.77 mg/g, respectively. The process of heavy metal ion forming a complex with humic acid: $H_mA \xrightarrow{-mH^+} A^{m-} \xrightarrow{+M^{n+}} MA^{n-m}$ is affected by the competition between H_mA dissociation and MA^{n-m} complex equilibrium (Li *et al.* 1997). At different pH, the degree of dissociation of carboxyl groups and phenolic hydroxyl groups contained in humic acid varies. Research has shown that pH greatly affects the complexation reaction between humic acid and metals, and its complexing ability and stability increase with increasing pH (Hu *et al.* 2017). When pH < 4.5, the removal of Mn(II) by IHA increased rapidly with the increase of pH, from 23.17% at pH = 2.5 to 54.87% at pH = 4.5, which may be because when the pH is at lower levels, the high concentration of H^+ in the solution is more competitive with the adsorption sites than Mn(II), and it more easily reacts with the active groups on the surface of humic acid, so that the metal ions are easily dissociated from the complex. When the pH is 4.5–7.5, the removal efficiency increases slowly. On the one hand, the adsorption of H^+ decreases and is released; at the same time, the H^+ on the functional groups such as carboxyl

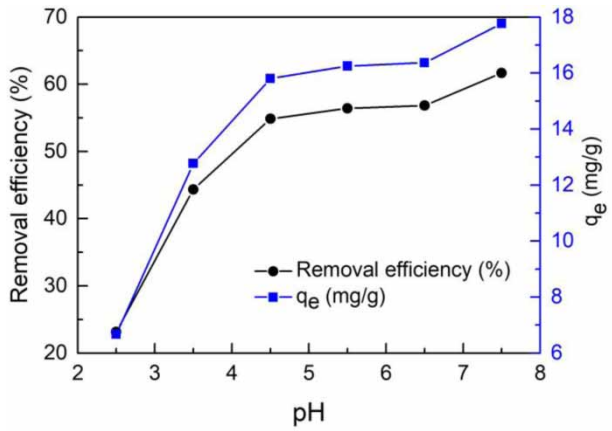

Figure 1 | The effect of pH on Mn(II) adsorption by IHA.

group and hydroxyl group is also dissociated; therefore, the negative charge on the humic acid increases and the adsorption sites increase (Ding *et al.* 2019), so that the humic acid and Mn(II) can undergo a complex reaction to reduce the free Mn(II) concentration in the solution. Also, the active functional group of humic acid tends to complex with manganese ions at higher pH, which is more conducive to the formation of humic acid-manganese complexes, thereby reducing the concentration of Mn(II) in solution (Barnie *et al.* 2018).

Effect of adsorbent dose on Mn(II) removal

Under the conditions of Mn(II) mass concentration of 100 mg/L, pH = 5.5, and temperature of 298.15 K, the effect of the dose of IHA (0.2–1.2 g) on Mn (II) removal was investigated (Figure 2).

It can be seen from the figure that with the increased dose of IHA, the removal efficiency of Mn(II) gradually increases, and the adsorption capacity gradually decreases. At low dose (0.20–0.80 g), the removal efficiency increased rapidly from 19.79% to 50.43%, with the adsorption capacity decreasing by 13.25 mg/g. This is because insolubilized humic acid contains a large number of active functional groups, in which the hydrogen in the functional groups such as -COOH and -OH is ionized to make it negatively charged (Basu *et al.* 2019). The negatively charged colloid has a strong binding capacity with the metal Mn(II) in the solution (Wei *et al.* 2019), so when the dose is gradually increased, the effective adsorption sites also relatively increase, so that the removal efficiency of manganese ions in the solution gradually increases. When the dose was 0.80–1.20 g, the removal efficiency increased slowly from 50.43% to 58.7%, and the adsorption capacity decreased by 4.4 mg/g. When the dose is high, the effective adsorption site is surrounded by a large number of insolubilized humic acid particles, and the electrostatic repulsion force between particles increases (Biswas *et al.* 2020), resulting in a decrease in the removal. However, due to the strong adsorption capacity of IHA, at high dose, a large number of adsorption sites can still effectively capture manganese ions (Cheng *et al.* 2015), thereby forming a complex of humic acid and manganese through coordination complexation, effectively reducing free manganese ions in solution.

Influence of initial Mn(II) concentration

The simulated surface water sample was adjusted to pH = 5.5, and insolubilized humic acid with a dry weight of 1.00 g was added into a series of simulated surface water samples containing Mn(II) of different concentrations (10–200 mg/L). The adsorption experiments were carried out at 298.15 K, 308.15 K and 318.15 K, and the effect of initial concentration of Mn(II) on the adsorption effect of IHA was studied (Figure 3).

As shown in Figure 3, both the temperature and initial concentration of the adsorption reaction will affect the adsorption performance of the adsorbent. At the same temperature, with the increase of the initial Mn(II) concentration in the solution, the removal efficiency of manganese by IHA decreased, while the adsorption capacity increased. In addition, at the same initial concentration of Mn(II), with the gradual increase of temperature, the removal efficiency of IHA on Mn(II) is also gradually improved. It can be seen that higher temperature is conducive to the removal of Mn(II) by IHA, which is assumed to be an endothermic reaction. When the concentration of Mn (II) is low, the

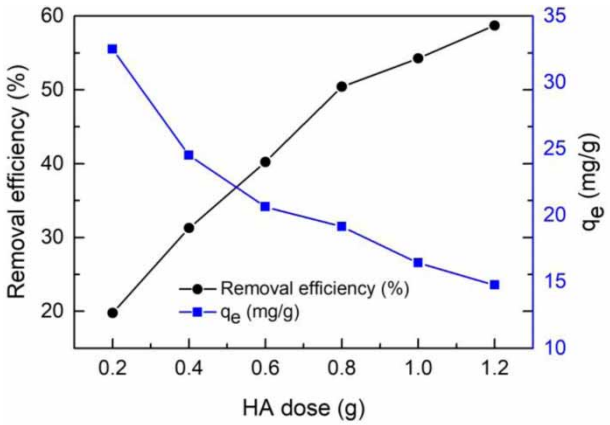

Figure 2 | The effect of IHA dose on Mn(II) adsorption by IHA.

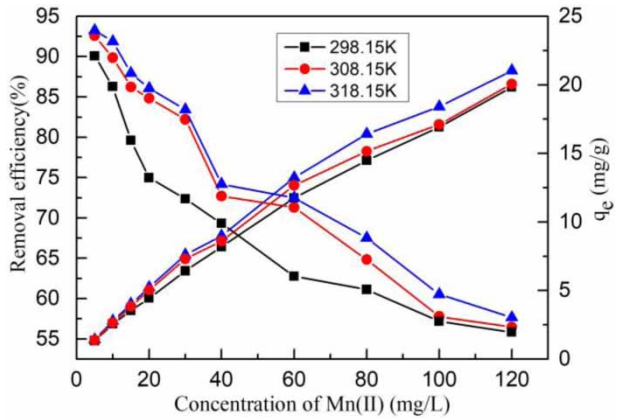

Figure 3 | Influence of Mn(II) concentrations on Mn(II) adsorption by IHA.

humic acid with negative charge combines with the Mn(II) with positive charge, and the free Mn(II) in the solution is surrounded by a large number of adsorption points with opposite charge, so the removal is high. After the initial stage, which depends on the concentration of Mn(II), the system slowly forms a stable complex of humic acid-Mn(II). When the concentration of Mn(II) is high, the active sites on the surface of the humic acid are occupied by a large number of Mn(II), and gradually reach saturation. At the same time, the increase of the positive charge on the surface of humic acid molecules causes a repulsive force and reduces the complexing ability of humic acid with Mn(II) (Li *et al.* 2019). Studies have shown that when the concentration of metal ions is high, the precipitation of humic acid-Mn(II) complex will occur, which affects the molecular structure of humic acid and reduces its reaction with Mn(II) (Engebretson & von Wandruszka 1998).

Adsorption kinetics

Aliquots of insolubilized humic acid with dry weights of 0.6, 0.8, 1.0 and 1.2 g were added to a series of simulated surface water samples containing Mn(II) with an initial concentration of 100 mg/L. The pH of the solution was adjusted to 5.5, and the adsorption kinetics experiment was carried out.

Figure 4 shows the relationship between the removal of Mn(II) and the adsorption time. The efficiency of removal of Mn(II) by IHA with the increase of contact time, and a higher removal efficiency can be obtained in a shorter time. Then with the increase of reaction time, the removal efficiency of IHA to Mn(II) increased slowly, the effective sites were occupied by Mn(II) gradually, and finally reached the adsorption equilibrium (Yang *et al.* 2014). The extremely fast adsorption rate in the initial stage indicates the strong affinity of IHA for Mn(II), which may be due to the presence of a large number of functional groups (Guo *et al.* 2017). At the same time, the dose of IHA has a significant effect on the process of reaching equilibrium in the adsorption reaction. When the dose is 0.6, 0.8 g, the time required to reach equilibrium is 300, 420 min, respectively; while the dose of IHA was 1.0 and 1.2 g, the time to reach adsorption equilibrium was 240 min. It can be seen that with the increase of the dose, the time for the completion of the adsorption reaction is also reduced, leading to a more rapid equilibrium for the adsorption reaction.

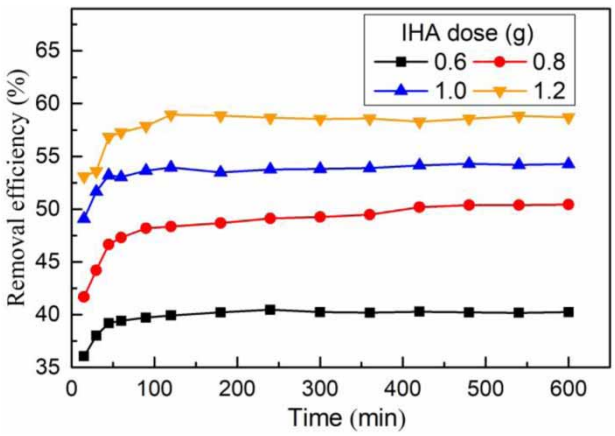

Figure 4 | The effect of contact time on the Mn(II) adsorption by IHA.

In order to further study the adsorption kinetics for Mn(II) on insolubilized humic acid, the pseudo-first-order kinetics model (4), pseudo-second-order kinetics model (5) and Weber-Morris model (internal diffusion model) (6) were used to fit the adsorption data.

$$\ln(q_e - q_t) = lnq_e - K_1 t \tag{4}$$

$$\frac{t}{q_t} = \frac{1}{k_2 q_e^2} + \frac{t}{q_e} \tag{5}$$

$$q_t = K_i t^{\frac{1}{2}} + c \tag{6}$$

where q_e and q_t represent the adsorption capacity (mg/g) for Mn(II) by the adsorbent at equilibrium and any time, respectively ; K_1 and K_2 are the adsorption rate constants of the pseudo-first order kinetic and the pseudo-second order kinetic, respectively; Ki is the internal diffusion rate constant (mg/(g·Min$^{1/2}$)); C is the thickness constant related to the boundary layer.

The results of the fit to the adsorption kinetic model are shown in Figures 5 and 6 and Table 1. It can be seen from Figure 5 that the pseudo-first-order kinetic model fits the experimental data well in the initial rapid adsorption stage, but gradually deviates from the curve as the adsorption stage slows (Li *et al.* 2008). It can be seen from Figure 5 and the parameters in Table 1 that under the condition that the dose of IHA is 0.6, 0.8, 1.0 and 1.2 g, the simulation of the humic acid adsorption Mn(II) process by the pseudo-second-order adsorption kinetic model is better than that by the pseudo-first-order adsorption kinetic model, and the equilibrium adsorption capacities q_e obtained by the pseudo-second-order kinetic equation are 20.77, 19.04, 16.45 and 14.82 mg/g respectively, which are closer to the measured values. It shows that the pseudo-second-order kinetic model can better reflect the adsorption process of IHA to Mn(II), and it is speculated that the adsorption process is mainly chemical adsorption (Huang *et al.* 2009; Li *et al.* 2011).

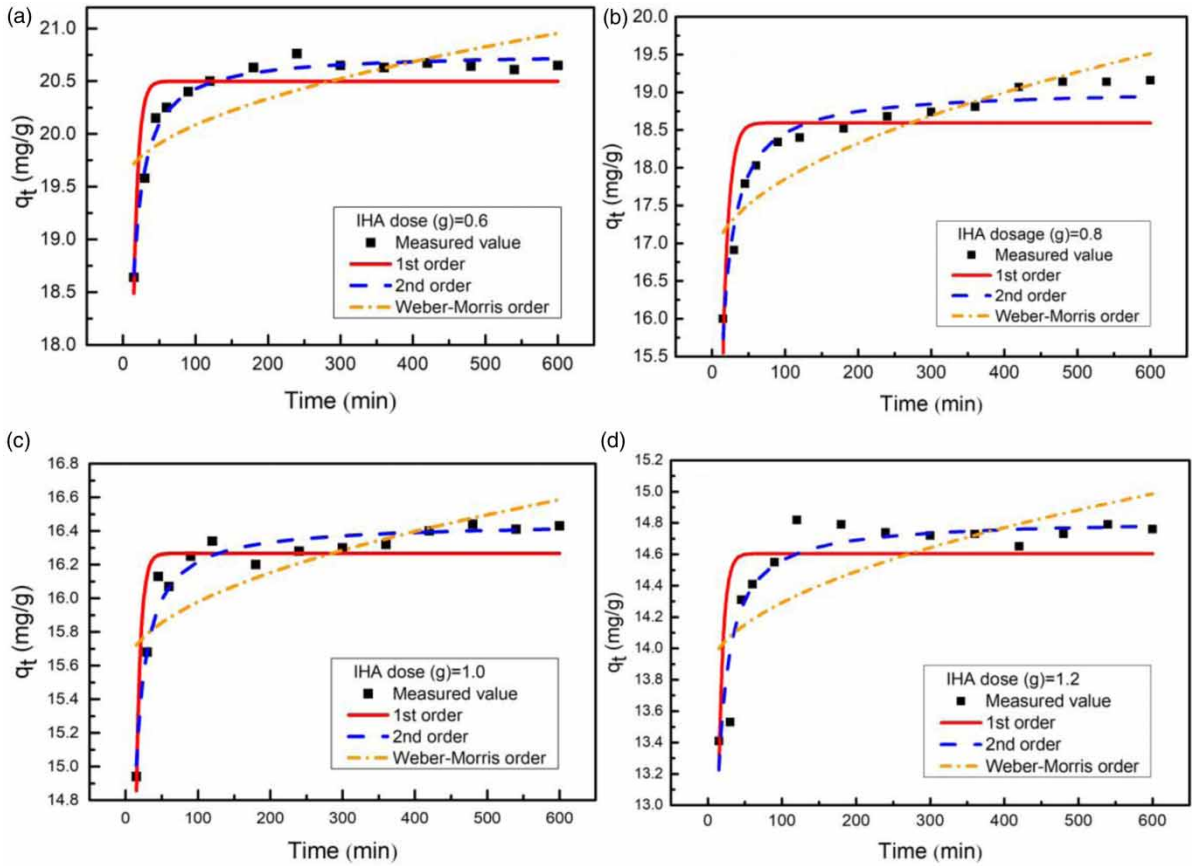

Figure 5 | Kinetic curves for different doses of IHA in the adsorption of Mn(II).

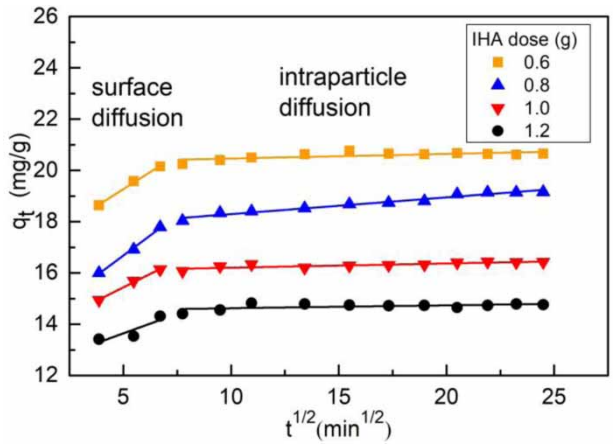

Figure 6 | Intraparticle diffusion model plots of Mn(II) adsorption on IHA.

It can be seen from the fitting curve of the internal diffusion model in Figure 6 that under different doses of IHA, the fitting of q_t to $t^{1/2}$ can be divided into two stages. In the initial stage, a large number of vacant active sites on IHA can be used to adsorb Mn(II); at this time, the adsorption reaction is mainly controlled by the ion exchange between Mn(II) and the functional groups on the surface of IHA and the diffusion of the external liquid membrane. The second stage is the slow adsorption; that is, as the binding sites are gradually occupied, a concentration gradient will form between the surface and the interior of the humic acid, which promotes the diffusion of Mn(II) into the interior of the humic acid molecule, and the adsorption rate is controlled by the intraparticle diffusion rate (Yang *et al.* 2018). From the different slopes of the first and second stages, it is known that there is a gradual stage in the adsorption process, the surface adsorption process is controlled by the thickness of the boundary layer. The internal diffusion rate constant Ki_2 is much smaller than Ki_1, which shows that the internal diffusion rate of particles is slow (Li *et al.* 2013b). Besides, the curve of q_t to $t^{1/2}$ is double-line in the whole time range, and the fitting curve does not pass through the origin, which shows that the adsorption process is not only affected by the internal diffusion of particles, but also under the common control of other adsorption stages (Li *et al.* 2013b). The adsorption

Table 1 | Kinetic parameters of Mn(II) adsorption on IHA

		m(IHA)/g			
model	**Parameter**	**0.6**	**0.8**	**1.0**	**1.2**
Pseudo-first-order model	q_e	20.49861	18.59564	16.26641	14.60372
	K_1	0.15482	0.12049	0.16305	0.1573
	R^2	0.76762	0.62763	0.80087	0.50704
Pseudo-second-order model	q_e	20.77106	19.04171	16.45022	14.82342
	K_2	0.02849	0.01666	0.04214	0.03732
	R^2	0.98328	0.95644	0.95741	0.87555
Weber-Morris model	Ki_1	0.53431	0.62701	0.42106	0.30472
	C_1	16.59632	13.5434	13.32928	12.11874
	R^2	0.99196	0.99092	0.99215	0.57744
	Ki_2	0.01794	0.06517	0.01656	0.01143
	C_2	20.28162	17.64273	16.03645	14.50845
	R	0.42392	0.96276	0.69052	0.21228

rate of Mn(II) by IHA is determined by the boundary layer effect and the external mass transfer effect (Dong & Wang 2016).

Adsorption isotherms

The adsorption isotherm is of great significance for the study of the interaction between adsorbent and adsorbate and the evaluation of the adsorption performance of adsorbent (Zhang *et al.* 2018). According to the results of adsorption kinetics, the adsorption of Mn(II) by insolubilized humic acid reached equilibrium at 240 min. In order to ensure sufficient adsorption, 24 h was chosen as the adsorption equilibrium time. Freundlich (7) and Langmuir (8) isotherm adsorption equations were used to analyze the data at 298.15 K, 308.15 K and 318.15 K (Figure 7(a) and 7(b) and Table 2). The Freundlich model is an empirical formula that is suitable for non-uniform multilayer adsorption (Piri *et al.* 2019), while the Langmuir model assumes that the adsorbent surface is uniform and is suitable for single-layer adsorption that occurs on the adsorbent surface (Saleh *et al.* 2017).

$$q_e = k_F C_e^{\frac{1}{n}} \tag{7}$$

$$\frac{1}{q_e} = \frac{1}{q_m} + \frac{1}{k_L q_m}\frac{1}{C_e} \tag{8}$$

where q_e and q_m are the equilibrium adsorption capacity and maximum adsorption capacity respectively (mg/g); k_F and k_L are the adsorption coefficients in Freundlich and Langmuir; Ce is the concentration of Mn(II) at the adsorption equilibrium (mg/L) ; 1/n is the parameter related to adsorption capacity and adsorption intensity in Freundlich.

From Figure 7(a) and 7(b), it can be seen that both Freundlich and Langmuir equations can fit the adsorption

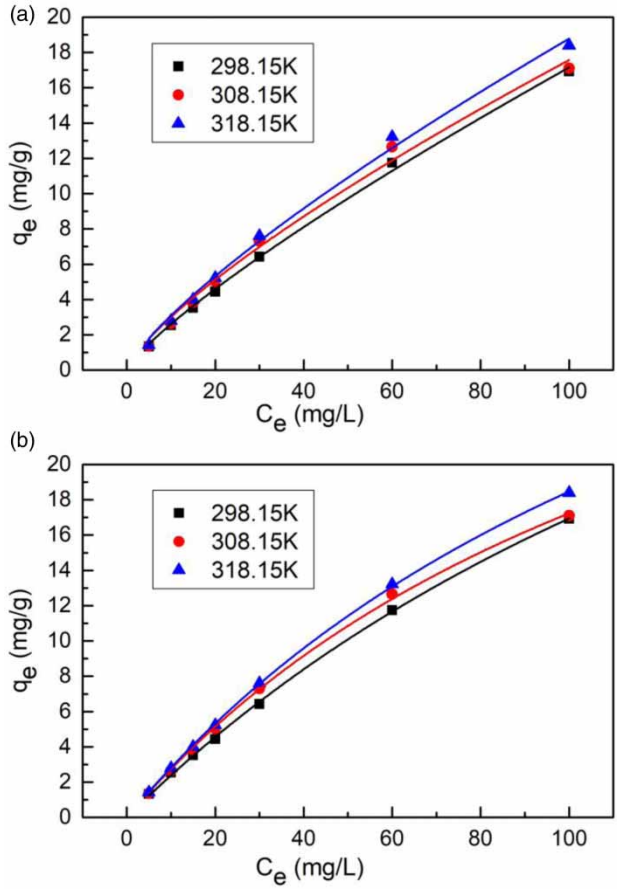

Figure 7 | Langmuir (a) and Freundlich (b) isotherms of for Mn(II) by IHA.

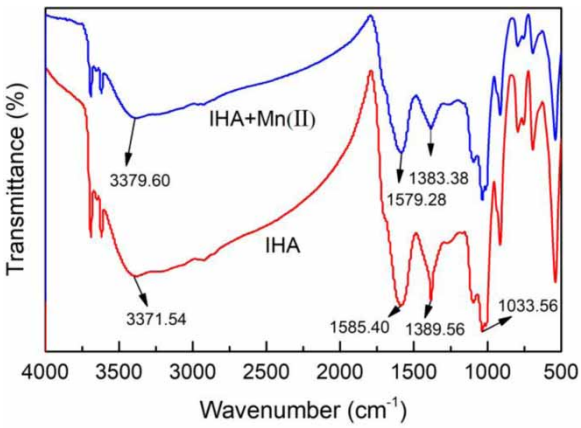

Figure 8 | The FTIR spectra of IHA before and after Mn(II) adsorption.

process well. The correlation coefficient R^2 in both models is greater than 0.99, which indicates that under this experimental condition, single-layer adsorption and heterogeneous surface adsorption coexist, and the adsorption process of insolubilized humic acid on Mn(II) is complicated, involving a variety of adsorption mechanisms (Zheng *et al.* 2018). Under the temperature conditions of 298.18 K, 308.18 K, and 318.18 K, the maximum adsorption capacity of insolubilized humic acid for Mn(II) fitted by the Langmuir model for manganese ions is 41.81 and 48.30 and 52.87 mg/g, respectively, which is close to the actual adsorption capacity. At the same time, it can be seen that the increase of temperature is conducive to the adsorption reaction, the main reason being that the temperature increase causes the adsorption equilibrium to move to the right. In addition, the values of R_L in the Langmuir model and 1/n in the Freundlich model are between 0 and 1, indicating that insolubilized humic acid has a higher affinity for Mn(II) (Acar & Malkoc 2004; Zhang *et al.* 2018).

Thermodynamic analysis

The adsorption thermodynamics parameters ΔG, ΔH and ΔS are obtained by fitting the experimental data obtained at different temperatures, so as to better understand the influence of temperature on the adsorption process. ΔG, ΔH, ΔS and k_d are calculated by Equations (9)–(11), respectively.

$$\Delta G = -RT\ln k_d \tag{9}$$

$$\ln k_d = \frac{\Delta S}{R} - \frac{\Delta H}{RT} \tag{10}$$

$$k_d = \frac{q_e}{C_e} \tag{11}$$

where ΔG is Gibbs free energy (KJ/mol), R is the gas constant (J/(mol • K)), k_d is the thermodynamic equilibrium constant, ΔH is the enthalpy change (KJ/mol), and ΔS is the entropy change (KJ/(mol • K)); linearly fit ln k_d to 1/T by formula (10) to obtain ΔH, ΔS.

The results of adsorption thermodynamic parameters are shown in Table 3. It can be seen from $\Delta G > 0$ that the adsorption of Mn(II) by insolubilized humic acid is a non-spontaneous reaction process, $\Delta H > 0$ indicates that the adsorption process is an endothermic reaction (Kimuro *et al.* 2019), and the increase of temperature is conducive to the adsorption process, which also confirms that the adsorption capacity of IHA increases gradually with the increase of temperature during the experiment. When the initial concentration of Mn(II) is 5 mg/L, $\Delta G < 0$, which

Table 3 | Thermodynamic parameters for the adsorption of Mn(II) on IHA

			ΔG		
Ce	ΔH	ΔS	298.15 K	308.15 K	318.15 K
5	2.5471	−0.0025	3.2767	3.3164	3.3345
10	3.7225	0.0009	3.3832	3.3924	3.3733
15	5.2509	0.0053	3.5829	3.4983	3.4891
20	6.8362	0.0101	3.7314	3.5404	3.5467
30	7.0216	0.0104	3.8194	3.6204	3.6289
60	4.9180	0.0027	4.0420	3.9856	4.0002
100	3.4755	0.0034	4.4031	4.5244	4.4773

Table 2 | Fitting parameters of adsorption isotherm

	Freundlich model			Langmuir model		
Temperature/K	1/n	K_F	R^2	q_m	K_L	R^2
298.15	0.7663	0.5153	0.9921	41.8145	0.0070	0.9991
308.15	0.7839	0.5079	0.9950	48.2983	0.0061	0.9997
318.15	0.8181	0.3962	0.9980	52.8676	0.0047	0.9994

indicates that the degree of freedom of Mn(II) decreases on the solid-liquid interface, and Mn(II) initially occupies the effective adsorption site on HA at low concentration, but with the increase of concentration $\Delta G > 0$, which indicates that the disorder of solid-liquid interface increases during the adsorption of Mn(II) by IHA. Since the entry of Mn(II) into the liquid phase is a process of increasing the degree of freedom, the rate of increase is greater than the rate of decrease in the degree of freedom caused by the adsorption of Mn(II) on IHA. The water molecules on the IHA surface dissociate due to adsorption, which leads to the increase of free molecules in the whole system (Yang *et al.* 2018).

CHARACTERIZATION

FTIR analysis

The FTIR spectroscopy of the IHA before sorption and after sorption were obtained in the wavenumber range of 4,000–500 cm^{-1}. The broad and strong characteristic absorbance peaks of IHA at 3,371.54 cm^{-1} are mainly caused by -OH stretching vibration on the carboxyl group, alcohol hydroxyl group and phenolic hydroxyl group (Chen *et al.* 2015). The characteristic peak of the functional groups changed after IHA adsorbs Mn(II). -OH located at the wavelength of 3,371.54 cm^{-1} can play a hydrogen bonding role when IHA adsorbs Mn(II) (Boguta *et al.* 2019); after absorption, the intensity of the -OH stretching vibration peak in the complex of humic acid and manganese ions weakened, indicating that Mn(II) reacted with -OH on IHA (Erdogan *et al.* 2007). It is speculated that the mechanism of insolubilized humic acid adsorption on Mn(II) includes surface hydroxyl exchange. At 1,579.28 and 1,383.38 cm^{-1}, they are the antisymmetric stretching vibration peak and the symmetric stretching vibration peak of COO-, respectively. Compared with before and after adsorption, it is speculated that the carboxyl group participated in the complexation, and part of the COOH was transformed into the carboxylate COO- (Boguta & Sokołowska 2016). 1,033.56 cm^{-1} is the characteristic peak of C-O low strength stretching vibration of ether (Zhang *et al.* 2015). The change in functional groups indicates that the carboxyl group and hydroxyl group participate in the adsorption of Mn(II) on IHA. The present study agrees with the findings of Md. Aminul Islam *et al.* (Islam *et al.* 2020). The adsorption of Mn(II) on IHA includes chemical and physical effects, and combined with adsorption kinetics studies, this process is mainly chemical adsorption.

SEM-EDS analysis

Scanning electron microscope was used to observe the surface morphology of insolubilized humic acid before and after adsorption. Figure 9(a) is a sample obtained by adding IHA to a deionized aqueous solution containing no Mn(II), after the same treatment time as the Mn(II) adsorption experiment. It can be seen from Figure 9 that the appearance and morphology of IHA before and after adsorption of manganese ions are significantly changed. It can be seen from Figure 9(a) that the surface of the adsorbent insolubilized humic acid is uneven, rough, and clustered between the particles, which increases the specific surface area of the adsorbent and helps it adsorb metal manganese ions (Zhang *et al.* 2020). Comparing Figure 9(a) and 9(b), it can be seen that after adsorption, insolubilized humic acid loses the full cluster structure formed by large particles, thus presenting the form of small particles, and a large number of small particles and fragments are produced. This is due to the adsorption reaction between Mn(II) and insolubilized humic acid, and the functional groups on the surface of humic acid participate in the adsorption of Mn(II) (Jiang *et al.* 2015; Chen *et al.* 2020). EDS spectra of

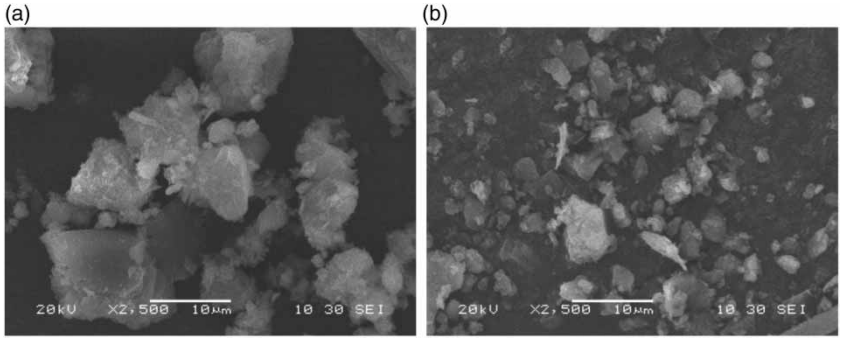

Figure 9 | SEM mapping micrographs of IHA (a) and IHA-Mn(II) (b).

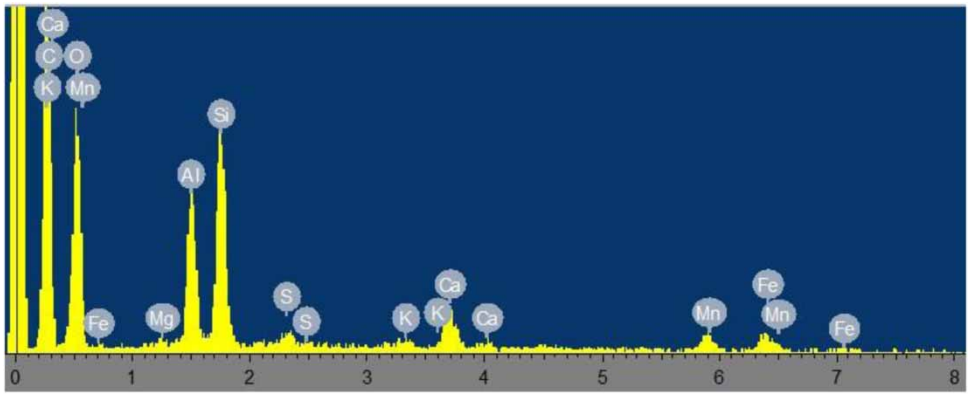

Figure 10 | EDS image of IHA-Mn(II).

HA-Mn(II) complex surface is shown in Figure 10. It can be seen that the content of C element in the sample is extremely high, and the appearance of elements such as Al and Si may be caused by impurities in the commercially available humic acid (Wang *et al.* 2020). At the same time, the appearance of Mn element in the spectrum shows that IHA successfully adsorbed Mn(II) from aqueous solution.

CONCLUSION

In this study, insoluble humic acid (IHA), a natural organic substance with abundant reserves in nature, was used to remove Mn(II) from aqueous solutions. Batch adsorption experiments showed that IHA has an excellent adsorption effect on Mn(II), and pH had a significant impact on the adsorption performance of IHA. Under the condition of pH = 5.6 and temperature of 298.15 K, the maximum adsorption capacity of IHA was 52.87 mg/g. According to the results of adsorption kinetics and isotherm adsorption characteristics of IHA for Mn(II), the adsorption process conformed to the pseudo-second-order model and Langmuir model, and the adsorption of Mn(II) on IHA was mainly a chemical reaction. Thermodynamic analysis showed that the adsorption is a non-spontaneous endothermic reaction. FTIR analysis showed that the functional groups on IHA reacted with Mn(II). Due to the advantages of low-cost and eco-friendliness, IHA can be feasible for some certain practical wastewater treatment.

ACKNOWLEDGEMENTS

This work was supported by the National Natural Science Foundation of China (No. 41973078) and the Ministry of Education in China Project of Humanities and Social Science (2019JJ40081).

DATA AVAILABILITY STATEMENT

All relevant data are included in the paper or its Supplementary Information.

REFERENCES

Acar, F. N. & Malkoc, E. 2004 The removal of chromium(VI) from aqueous solutions by *Fagus orientalis* L. *Bioresource Technology* **94** (1), 13–15. https://doi.org/10.1016/j.biortech.2003.10.032.

Barnie, S., Zhang, J., Wang, H., Yin, H. & Chen, H. 2018 The influence of pH, co-existing ions, ionic strength, and temperature on the adsorption and reduction of hexavalent chromium by undissolved humic acid. *Chemosphere* **212**, 209–218. doi:10.1016/j.chemosphere.2018.08.067.

Basu, H., Saha, S., Mahadevan, I. A., Pimple, M. V. & Singhal, R. K. 2019 Humic acid coated cellulose derived from rice husk: a novel biosorbent for the removal of Ni and Cr. *Journal of Water Process Engineering* **32**, 100892. https://doi.org/10.1016/j.jwpe.2019.100892.

Biswas, S., Mohapatra, S. S., Kumari, U., Meikap, B. C. & Sen, T. K. 2020 Batch and continuous closed circuit semi-fluidized bed operation: removal of MB dye using sugarcane bagasse biochar and alginate composite adsorbents. *Journal of Environmental Chemical Engineering* **8** (1), 103637. https://doi.org/10.1016/j.jece.2019.103637.

Boguta, P. & Sokołowska, Z. 2016 Interactions of Zn(II) ions with humic acids isolated from various type of soils. Effect of pH, Zn concentrations and humic acids chemical properties. *PLoS One* **11** (4), e0153626. https://doi.org/10.1371/journal.pone.0153626.

Boguta, P., D'Orazio, V., Senesi, N., Sokołowska, Z. & Szewczuk-Karpisz, K. 2019 Insight into the interaction mechanism of iron ions with soil humic acids. The effect of the pH and

chemical properties of humic acids. *Journal of Environmental Management* **245**, 367–374. https://doi.org/10.1016/j.jenvman.2019.05.098.

Chen, T., Zhou, Z., Xu, S., Wang, H. & Lu, W. 2015 Adsorption behavior comparison of trivalent and hexavalent chromium on biochar derived from municipal sludge. *Bioresource Technology* **190**, 388–394. https://doi.org/10.1016/j.biortech.2015.04.115.

Chen, L., Zhu, Y., Luo, H. & Yang, J. 2020 Characteristic of adsorption, desorption, and co-transport of vanadium on humic acid colloid. *Ecotoxicology and Environmental Safety* **190**, 110087. https://doi.org/10.1016/j.ecoenv.2019.110087.

Cheng, L., Li, X. U., Luo, T., Zhang, B. & Liu, G. 2015 Adsorption thermodynamics and kinetics of Cr(VI) of nanoscale humic acid. *Chemical Industry & Engineering Progress (China)* **34** (06), 1792–1798. doi:10.16085/j.issn.1000-6613.2015.06.046.

Ding, H., Tang, L., Nie, Y. & Ji, H. 2019 Characteristics and interactions of heavy metals with humic acid in gold mining area soil at a upstream of a metropolitan drinking water source. *Journal of Geochemical Exploration* **200**, 266–275. https://doi.org/10.1016/j.gexplo.2018.09.003.

Dong, S. & Wang, Y. 2016 Characterization and adsorption properties of a lanthanum-loaded magnetic cationic hydrogel composite for fluoride removal. *Water Research* **88**, 852–860. https://doi.org/10.1016/j.watres.2015.11.013.

El-Eswed, B. & Khalili, F. 2006 Adsorption of Cu(II) and Ni(II) on solid humic acid from the Azraq area, Jordan. *Journal of Colloid and Interface Science* **299** (2), 497–503. https://doi.org/10.1016/j.jcis.2006.02.048.

Engebretson, R. & von Wandruszka, R. 1998 Kinetic aspects of cation-enhanced aggregation in aqueous humic acids. *Environmental Science & Technology* **32** (4), 488–493. doi:10.1021/es970693s.

Erdogan, S., Baysal, A., Akba, O. & Hamamci, C. 2007 Interaction of metals with humic acid isolated from oxidized coal. *Polish Journal of Environmental Studies* **16**, 671–675.

Guo, S., Jiao, P., Dan, Z., Duan, N., Chen, G. & Zhang, J. 2017 Preparation of L-arginine modified magnetic adsorbent by one-step method for removal of Zn(II) and Cd(II) from aqueous solution. *Chemical Engineering Journal* **317**, 999–1011. https://doi.org/10.1016/j.cej.2017.02.136.

He, Z. L., Yang, X. E. & Stoffella, P. J. 2005 Trace elements in agroecosystems and impacts on the environment. *Journal of Trace Elements Medicine and Biology* **19** (2–3), 125–140. https://doi.org/10.1016/j.jtemb.2005.02.010.

Hou, D., Zhang, P., Wei, D., Zhang, J., Yan, B., Cao, L., Zhou, Y. & Luo, L. 2020 Simultaneous removal of iron and manganese from acid mine drainage by acclimated bacteria. *Journal of Hazardous Materials* **396**, 122631. https://doi.org/10.1016/j.jhazmat.2020.122631.

Hu, E., Zhang, Y., Wu, S., Wu, J., Liang, L. & He, F. 2017 Role of dissolved Mn(III) in transformation of organic contaminants: non-oxidative versus oxidative mechanisms. *Water Research* **111**, 234–243. https://doi.org/10.1016/j.watres.2017.01.013.

Huang, G., Shi, J. X. & Langrish, T. A. G. 2009 Removal of Cr(VI) from aqueous solution using activated carbon modified with nitric acid. *Chemical Engineering Journal* **152** (2–3), 434–439. https://doi.org/10.1016/j.cej.2009.05.003.

Huang, M., Zhang, Y., Xiang, W., Zhou, T., Wu, X. & Mao, J. 2019 Efficient adsorption of Mn(II) by layered double hydroxides intercalated with diethylenetriaminepentaacetic acid and the mechanistic study. *Journal of Environmental Sciences* **85**, 56–65. https://doi.org/10.1016/j.jes.2019.04.011.

Islam, M., Morton, D., Johnson, B. & Angove, M. 2020 Mechanism of humic acid (HA) adsorption onto manganese oxides and boehmite. In: *Conference on Recent Advances in Chemistry (ICRAC-2020)*. Department of Chemistry, Jagannath University, Dhaka, Bangladesh. doi:10.13140/RG.2.2.11838.64320.

Jiang, H. Y., Zhou, S. K., Zeng, G. M., Liu, Y. J., Hua, L. I. & Ouyang, S. L. 2015 Thermodynamics and kinetics of the adsorption of insolubilized humic acid to uranium(VI) ions. *Journal of Safety & Environment (China)* **15** (01), 193–198. doi:10.13637/j.issn.1009-6094.2015.01.040.

Jiang, F., Ren, B., Hursthouse, A. & Zhou, Y. 2018 Trace metal pollution in topsoil surrounding the Xiangtan manganese mine area (South-Central China): source identification, spatial distribution and assessment of potential ecological risks. *International Journal of Environmental Research & Public Health* **15** (11), 2412. https://doi.org/10.3390/ijerph15112412.

Khalili, F. & Al-Banna, G. 2015 Adsorption of uranium(VI) and thorium(IV) by insolubilized humic acid from Ajloun soil–Jordan. *Journal of Environmental Radioactivity* **146**, 16–26. https://doi.org/10.1016/j.jenvrad.2015.03.035.

Kimuro, S., Kirishima, A., Kitatsuji, Y., Miyakawa, K., Akiyama, D. & Sato, N. 2019 Thermodynamic study of the complexation of humic acid by calorimetry. *The Journal of Chemical Thermodynamics* **132**, 352–362. https://doi.org/10.1016/j.jct.2019.01.011.

Lan, S., Wang, X., Xiang, Q., Yin, H., Tan, W., Qiu, G., Liu, F., Zhang, J. & Feng, X. 2017 Mechanisms of Mn(II) catalytic oxidation on ferrihydrite surfaces and the formation of manganese (oxyhydr)oxides. *Geochimica et Cosmochimica Acta* **211**, 79–96. https://doi.org/10.1016/j.gca.2017.04.044.

Li, K., Liu, W. & Shao, Y. 1997 Adsorption of heavy metal ions on humic acid. *Environmental Pollution & Control* (01), 9–11. doi:10.15985/j.cnki.1001-3865.1997.01.004.

Li, Y., Yue, Q., Gao, B., Li, Q. & Li, C. 2008 Adsorption thermodynamic and kinetic studies of dissolved chromium onto humic acids. *Colloids and Surfaces B: Biointerfaces* **65** (1), 25–29. https://doi.org/10.1016/j.colsurfb.2008.02.014.

Li, Q., Sun, L., Zhang, Y., Qian, Y. & Zhai, J. 2011 Characteristics of equilibrium, kinetics studies for adsorption of Hg(II) and Cr(VI) by polyaniline/humic acid composite. *Desalination* **266** (1), 188–194. https://doi.org/10.1016/j.desal.2010.08.025.

Li, T., Tao, Q., Liang, C., Shohag, M. J. I., Yang, X. & Sparks, D. L. 2013a Complexation with dissolved organic matter and mobility control of heavy metals in the rhizosphere of hyperaccumulator *Sedum alfredii*. *Environmental Pollution* **182**, 248–255. https://doi.org/10.1016/j.envpol.2013.07.025.

Li, X., Qi, Y., Li, Y., Zhang, Y., He, X. & Wang, Y. 2013b Novel magnetic beads based on sodium alginate gel crosslinked by zirconium(IV) and their effective removal for Pb^{2+} in aqueous solutions by using a batch and continuous systems. *Bioresource Technology* **142**, 611–619. https://doi.org/10.1016/j.biortech.2013.05.081.

Li, Q., Xie, L., Jiang, Y., Fortner, J. D., Yu, K., Liao, P. & Liu, C. 2019 Formation and stability of NOM-Mn(III) colloids in aquatic environments. *Water Research* **149**, 190–201. https://doi.org/10.1016/j.watres.2018.10.094.

Manzak, A., Kurşun, C. & Yıldız, Y. 2017 Characterization of humic acid extracted from aqueous solutions with polymer inclusion membranes. *Journal of the Taiwan Institute of Chemical Engineers* **81**, 14–20. https://doi.org/10.1016/j.jtice.2017.10.024.

Oldham, V. E., Miller, M. T., Jensen, L. T. & Luther, G. W. 2017 Revisiting Mn and Fe removal in humic rich estuaries. *Geochimica et Cosmochimica Acta* **209**, 267–283. https://doi.org/10.1016/j.gca.2017.04.001.

Patil, D. S., Chavan, S. M. & Oubagaranadin, J. U. K. 2016 A review of technologies for manganese removal from wastewaters. *Journal of Environmental Chemical Engineering* **4** (1), 468–487. https://doi.org/10.1016/j.jece.2015.11.028.

Piri, M., Sepehr, E. & Rengel, Z. 2019 Citric acid decreased and humic acid increased Zn sorption in soils. *Geoderma* **341**, 39–45. https://doi.org/10.1016/j.geoderma.2018.12.027.

Saleh, T. A., Sarı, A. & Tuzen, M. 2017 Effective adsorption of antimony(III) from aqueous solutions by polyamide-graphene composite as a novel adsorbent. *Chemical Engineering Journal* **307**, 230–238. https://doi.org/10.1016/j.cej.2016.08.070.

Schulten, H. R. & Schnitzer, M. 1993 A state of the art structural concept for humic substances. *Science of Nature* **80** (1), 29–30. doi:10.1007/BF01139754.

Wang, X., Muhmood, A., Dong, R. & Wu, S. 2020 Synthesis of humic-like acid from biomass pretreatment liquor: quantitative appraisal of electron transferring capacity and metal-binding potential. *Journal of Cleaner Production* **255**, 120243. https://doi.org/10.1016/j.jclepro.2020.120243.

Wei, L., Li, J., Xue, M., Wang, S., Li, Q., Qin, K., Jiang, J., Ding, J. & Zhao, Q. 2019 Adsorption behaviors of Cu^{2+}, Zn^{2+} and Cd^{2+} onto proteins, humic acid, and polysaccharides extracted from sludge EPS: sorption properties and mechanisms. *Bioresource Technology* **291**, 121868. https://doi.org/10.1016/j.biortech.2019.121868.

Yang, G., Tang, L., Lei, X., Zeng, G., Cai, Y., Wei, X., Zhou, Y., Li, S., Fang, Y. & Zhang, Y. 2014 Cd(II) removal from aqueous solution by adsorption on α-ketoglutaric acid-modified magnetic chitosan. *Applied Surface Science* **292**, 710–716. https://doi.org/10.1016/j.apsusc.2013.12.038.

Yang, L. F., Liu, Z. R., Wang, Y., Yang, Q., Min, H. Q. & Liu, Y. N. 2018 Adsorption performance of thorium(IV) by insolubilized humic acid. *Fine Chemicals (China)* **35** (04), 662–667. doi:10.13550/j.jxhg.2018.04.021.

Yong, L., Bai, J., Duan, H. & Yin, X. 2017 Static magnetic field-assisted synthesis of Fe_3O_4 nanoparticles and their adsorption of Mn(II) in aqueous solution. *Chinese Journal of Chemical Engineering* **25** (1), 32–36. https://doi.org/10.1016/j.cjche.2016.05.034.

Zhang, J., Lv, B., Xing, M. & Yang, J. 2015 Tracking the composition and transformation of humic and fulvic acids during vermicomposting of sewage sludge by elemental analysis and fluorescence excitation–emission matrix. *Waste Management* **39**, 111–118. https://doi.org/10.1016/j.wasman.2015.02.010.

Zhang, W., Deng, Q., He, Q., Song, J., Zhang, S., Wang, H., Zhou, J. & Zhang, H. 2018 A facile synthesis of core-shell/bead-like poly(vinyl alcohol)/alginate@PAM with good adsorption capacity, high adaptability and stability towards Cu(II) removal. *Chemical Engineering Journal* **351**, 462–472. https://doi.org/10.1016/j.cej.2018.06.129.

Zhang, S., Song, J., Du, Q., Cheng, K. & Yang, F. 2020 Analog synthesis of artificial humic substances for efficient removal of mercury. *Chemosphere* **250**, 126606. https://doi.org/10.1016/j.chemosphere.2020.126606.

Zheng, C., Zheng, H., Wang, Y., Wang, Y., Qu, W., An, Q. & Liu, Y. 2018 Synthesis of novel modified magnetic chitosan particles and their adsorption performance toward Cr(VI). *Bioresource Technology* **267**, 1–8. https://doi.org/10.1016/j.biortech.2018.06.113.

First received 7 July 2020; accepted in revised form 31 July 2020. Available online 12 August 2020